Journal of Medicinal Chemistry

Article

Novel Inhibitors of Staphyloxanthin Virulence Factor in Comparison with Linezolid and Vancomycin versus Methicillin-Resistant, Linezolid-Resistant and Vancomycin-Intermediate Staphylococcus aureus Infections in vivo

Shuaishuai Ni, Hanwen Wei, Baoli Li, Feifei Chen, Yifu Liu, Wenhua Chen, Yixiang Xu, Xiaoxia Qiu, Xiaokang Li, Yanli Lu, Wenwen Liu, Linhao Hu, Dazheng Lin, Manjiong Wang, Xinyu Zheng, Fei Mao, Jin Zhu, Le-Fu Lan, and Jian Li

J. Med. Chem., **Just Accepted Manuscript** • DOI: 10.1021/acs.jmedchem.7b00949 • Publication Date (Web): 07 Sep 2017

Just Accepted

ACS Publications

Journal of Medicinal Chemistry is published by the American Chemical Society. 1155 Sixteenth Street N.W., Washington, DC 20036

Novel Inhibitors of Staphyloxanthin Virulence Factor in Comparison with Linezolid and Vancomycin *versus* Methicillin-Resistant, Linezolid-Resistant and Vancomycin-Intermediate *Staphylococcus aureus* Infections *in vivo*

Shuaishuai Ni[a, †], Hanwen Wei[a, †], Baoli Li[a, †], Feifei Chen[b], Yifu Liu[a], Wenhua Chen[a], Yixiang Xu[a], Xiaoxia Qiu[a], Xiaokang Li[a], Yanli Lu[a], Wenwen Liu[a], Linhao Hu[a], Dazheng Lin[a], Manjiong Wang[a], Xinyu Zheng[a], Fei Mao[a], Jin Zhu[a], Lefu Lan[b,*], Jian Li[a,*]

[a]Shanghai Key Laboratory of New Drug Design, School of Pharmacy, East China University of Science and Technology, Shanghai 200237, China

[b]State Key Laboratory of Drug Research, Shanghai Institute of Material Medical, Chinese Academy of Sciences, Shanghai 201203, China

[†]These authors contributed equally to this work.

*To whom correspondence should be addressed: jianli@ecust.edu.cn or llan@simm.ac.cn.

ABSTRACT

Our previous work (Wang, et al. *J. Med. Chem.* **2016**, *59*, 4831-4848) revealed that effective benzocycloalkane-derived staphyloxanthin inhibitors against methicillin-resistant *Staphylococcus aureus* (*S. aureus*) infections were accompanied by poor water solubility and high hERG inhibition and dosages (pre-administration). In this study, ninety-two chroman and coumaran derivatives as novel inhibitors have been addressed for overcoming deficiencies above. Derivatives **69** and **105** displayed the excellent pigment inhibitory activities and low hERG inhibition, along with the improvement of solubility by salt type selection. The broad and significantly potent antibacterial spectra of **69** and **105** were displayed firstly with normal administration in the livers and hearts in mice against pigmented *S. aureus* Newman, Mu50 (vancomycin-intermediate *S. aureus*) and NRS271 (linezolid-resistant *S. aureus*), compared with linezolid and vancomycin. In summary, both **69** and **105** have the potential to be developed as good antibacterial candidates targeting virulence factors.

INTRODUCTION

Drug-resistant bacteria have become one of the most serious health issues for global public health. *Staphylococcus aureus* (*S. aureus*) is a major Gram-positive pathogen that causes a series of diseases, from mild external infections to severe organ bacteremia, with rapid evolution of antibiotic resistance under the abuse of antibiotic drugs.[1-4] Methicillin-resistant *S. aureus* (MRSA)，the best-known pathogen, was reported first in 1961.[5] Other drug-resistant MRSA strains had been identified since[6-9]; in particular, the emergence of linezolid-resistant *S. aureus* (LRSA) and vancomycin-resistant *S. aureus* (VRSA) in hospitals have proved challenging to currently existing drugs since they have limited efficacy in these strains.[10-11] As issued by the US Centers for Disease Control and Prevention (CDC) in 2015, more than 23 thousand people died and more than 2 million got sick per year due to MRSA infections in the United States.[12] In 2017, the World Health Organization (WHO) grouped and stratified methicillin-resistant and vancomycin-intermediate and -resistant *S. aureus* in the high tier on the global priority list of antibiotic-resistant bacteria.[13] Consequently, the drug-resistant forms of MRSA strains have shrugged off the most powerful antibiotics. To decelerate the spread of antibiotic resistance, it is extremely urgent to facilitate the next class of chemotherapeutics with novel mechanisms of action.

The function of bacterial virulence factors is to strengthen the growth and survivability of *S. aureus* under stressful environments.[14] Targeting bacterial virulence factors is a magnetic approach to combatting pathogenesis without exerting immediate life-or-death pressure on the target bacterium, offering a promising

opportunity to creating new antibacterial molecules to prevent and treat infectious diseases.[15,16] Staphyloxanthin (STX), known as a golden carotenoid pigment distributed in *S. aureus*, the structure of which contains numerous conjugated double bonds to resist the reactive oxygen species (ROS) produced by neutrophils and macrophages, has been deemed an important virulence factor with antioxidant properties.[17-19] Therefore, blocking the STX biosynthetic pathway is an effective therapeutic strategy for complicated *S. aureus* infections.[20-25] Eric Oldfield and colleagues reported compound **1 (**BPH-652, Figure 1) in 2008, which could block the biosynthesis of STX by inhibition of the *S. aureus* dehydrosqualene synthase (CrtM) enzyme.[26-28] Diapophytoene desaturase (CrtN), another essential enzyme for catalyzing three sequential reactions during the biosynthesis of STX, was identified by our group as an appealing druggable target against pigmented *S. aureus* infections.[29]

A previous study by our group revealed that compound **2** (NTF, Figure 1), an FDA-approved antifungal agent, was capable of blocking the STX biosynthesis pathway of three MRSA strains by inhibiting CrtN.[29] Based on the structure of **2**, compound **3** (Figure 1) with benzofuranyl attached was investigated as a better CrtN inhibitor *in vitro* by replacing the naphthyl of NTF, which only exhibited slightly greater efficacy than **2** *in vivo*.[30] Combined with its high inhibition of hERG potassium channels, **3** had been restrained for development forward. Subsequently, a series of new benzocycloalkane derivatives was synthesized, among which more compounds showed remarkable pigment inhibitory activities than benzofuranyl

derivatives. In particular, benzocycloalkane derivative **4** (Figure 1) displayed excellent bioactivity *in vitro* and *in vivo*.[31] However, low water solubility, high hERG inhibition and administration at high dosages *in vivo* limited further development of **4**.

Figure 1

Herein, our work focused on the design, synthesis and evaluation of a CrtN inhibitor with new scaffolds, which not only demonstrated excellent activity against MRSA *in vitro* and *in vivo* at lower dosages, but also overcame the disadvantages of water solubility and hERG inhibition. Additionally, linezolid and vancomycin, the last-resort antimicrobial agents, were introduced for the first time as positive control drugs into a murine model of *S. aureus* abscess formation to evaluate the effectiveness of our new compounds intuitively.

DESIGN AND SYNTHESIS

We had found that benzocycloalkane derivatives possessed potent pigment inhibitory activity *in vitro* and *in vivo.* However, the poor water solubility of the benzocycloalkane skeleton, along with strong hERG inhibition, limited their further development. As shown in Figure 2, benzocycloalkane derivative **5** exhibited more significant potency (IC_{50} = 1.9 nM) than **4** (IC_{50} = 4.1 nM) in a previous report but was blocked by poor water solubility (0.69 mg/mL)[31] and strong hERG inhibition (IC_{50} = 3.2 μM, Table 4), though it was valuable for further evaluation as a lead compound. Primarily, structural modification a general strategy was utilized to promote the solubility in this study, due to its conciseness and efficiency. Additionally, in order to improve its water solubility and maintain its potency with fewer changes

simultaneously, it is rational to insert a hydrophilic oxygen into the cycloalkane of **5**. Next, we designed and synthesized **24** by replacing benzocycloalkane with a *chroman* segment, which exhibited excellent pigment inhibitory activity (IC_{50} = 4.6 ± 0.2 nM) and improved water solubility (13.2 mg/mL, about 20 folds increase). Emboldened by the initial consequences of **24**, compound **62**, containing the *coumaran* segment as the other new skeleton, was synthesized, presenting comparable activity and solubility (IC_{50} = 2.0 ± 0.2 nM, 14.6 mg/mL), and the strategy of scaffold hopping is obviously responsible. Then, we proposed that anchoring core structures (*chroman* segment and *coumaran* segment) and introducing comprehensive modifications in other parts of the structure of **24/62** were the logical process to decrease hERG inhibition and maintain pigment inhibitory activity and solubility of derivatives, as shown in Figure 2. Therefore, the two series were identical in structural modification strategies, including: (1) incorporating hydrogen, cycloalkyls, heteroaryls and substituted aryls in region A; (2) replacing the N-methyl group with various steric alkyl groups R^3 (hydrogen, ethyl and isopropyl); and (3) changing the allyl linker with other fragments. These modifications generated ninety-two derivatives (**11-86**, **89-94** and **100-109**) in total combining either Series B or C.

Figure 2

The synthesis routes for the preparation of derivatives **11-86** were outlined in Scheme 1. The reduction of commercially available substituted cinnamaldehyde with sodium borohydride yielded intermediates **6a-p**, along with a bromination reaction by phosphorus tribromide to generate intermediates **7a-q**. The imidization of

coumaran-5-aldehyde with methylamine was further reduced by sodium borohydride, yielding intermediate **10a.** Then, target compounds **49**, **52**, **54**, **56-60**, **62**, **64**, **66**, **70-71**, **76-78**, and **82** were achieved by coupling **10a** with cinnamyl bromide **7a-q**. Two successive stages, including the Mizoroki-Heck reaction and deprotection in hydrochloric acid, were utilized to synthesize substituted cinnamaldehyde **8a-u**,[32] which were difficult to obtain from commercial resources. Intermediates **9a-u**, and target derivatives **50**, **51**, **53**, **55**, **61**, **63**, **65**, **67-69**, **72-75**, **79-81** and **83-86** were prepared using the same synthetic routes, as described above. In parallel, the preparation involved a nucleophilic aromatic substitution reaction between 3-propanediol and 2,5-dibromo-fluorobenzene to yield intermediate **10b**, followed by a bromination reaction to generate intermediate **10c**. The core ring scaffold **10d** was constructed by cyclization of **10c** with *n*-BuLi as the base at -70 °C, followed by *N*, *N*-dimethylformamide in *n*-BuLi at -70 °C again to yield intermediate **10e**.[33] Finally, intermediate **10f** and derivatives **11-48** were achieved.

Scheme 1

Derivatives **89-94** were prepared as described in scheme 2. Intermediates **87a** and **87b** were synthesized from **10e** and coumaran-5-aldehyde, respectively, with hydroxylamine hydrochloride using sodium hydroxide as the base at 40 °C, followed by hydrogenation with palladium hydroxide. Then, derivatives **89** and **90** were achieved by coupling **9j** with the two intermediates **87a-b**. Coumaran-5-aldehyde and **10e** were imidized with ethylamine or *iso*-propylamine, followed by reduction with

sodium cyanoborohydride to yield **88a-d**. Then, target derivatives **91-94** were achieved by coupling **88a-d** with **9j**.

Scheme 2

Scheme 3 outlines the synthetic strategy used for the synthesis of derivatives **100-109**. The synthesis of intermediate **95a** was initiated from **8j** via the Wittig reaction. The reduction of **95a** with diisobutyl aluminum hydride yielded intermediate **95b**, and followed by a bromination reaction to generate intermediate **95c**. The reduction of **8j** with sodium borohydride reduction to afford **96a**, followed by H_2 under the catalysis of Pd/C, yielded intermediates **96b**.[34] **96b**, which underwent bromination reaction by carbon tetrabromide to generate **96c**. After the Wittig reaction of methyl-(1-methyl-triphenyl-phosphoranylidene)-acetate with 4-phenyl-benzaldehyde, ester **97a** was obtained. The product was then reduced with diisobutyl aluminum hydride to yield intermediate **97b**, and followed by bromination to generate **97c**. Intermediate **98a** was generated from 4-phenyl-benzaldehyde by Wittig reaction and then underwent esterification, followed by reduction to intermediate **98b**,[35] and then the bromination of **98b** with phosphorous tribromide to **98c**. The starting material 4-phenyl-iodobenzene was reacted with O-TBDMS-2-propyny-1-ol via Sonogashira coupling, and the product **99a** was converted to intermediate **99b** by further deprotection. Then, the bromination of **99b** was performed with phosphorous tribromide to **99c**. The key intermediates **95c-99c** were reacted with **10a** or **10f** according to a procedure described previously to obtain derivatives **100-109**.

Scheme 3

RESULTS AND DISCUSSION

In total, ninety-two novel *chroman* and *coumaran* derivatives (**11-86**, **89-94** and **100-109**) were designed and synthesized. Their chemical structures are shown in Tables 1-3. These derivatives were synthesized through the routes outlined in Schemes 1-3, and the details of the synthetic procedures and structural characterization are described in the *Supporting Information*. All of the derivatives were confirmed to have ≥ 95% purity (Table S1, *Supporting Information*), and were identified with non-PAINS on the web at http://fafdrugs3.mti.univparis-diderot.fr/ recommended by editors from the ACS (American Chemical Society).[36]

In Vitro Pigment Inhibitory Activities of Derivatives 11-86, 89-94 and 100-109

Initial studies involved exploration around region A and systemic variation in R substitution for pigment inhibitory activities against *S. aureus* Newman. The results are summarized in Table 1. In general, substitution with various types of groups at the phenyl ring could remarkably affect pigment inhibitory activities, whereas methyl, cycloalkyls or heteroaryls displayed disappointing results. Previous studies preliminarily recognized that the electron-withdrawing groups and electron-donating groups at the phenyl ring might have minor effects on activity.[31] Herein, to investigate the SARs of the two new class of scaffolds systemically, more electron-withdrawing (fluoro, chloro, bromo, trifluoromethyl, difluoromethyl, nitro, phenyl, formate, cyan) and electron-donating groups (methyl, methoxyl, ethoxyl, *t*-butyl) were introduced at the phenyl ring. These results of modifications clearly demonstrated that there was no

relationship between potency and electronic effect, whereas the substituted positions at the phenyl ring substantially affected the activity. Subsequently, the substituted positions on the phenyl ring obviously affect the activity (Table 1). The substitution at the para-position showed more potency than the other two positions (**19/57-31/69** at para-position *vs* **32/70-37/75** at ortho-position *vs* **38/76-43/81** at meta-position). Relatively, a suitable bulk of substituents can significant increase inhibitory activity (**57** vs **58** vs **59**, **60** vs **61** vs **62** vs **63**). The substitution at the para-position with bromo, difluoromethyl, trifluoromethyl and phenyl (**21**, **23**, **24**, **31**, **62** and **69**) provided significant improvements in activities.

Next, benefit from good performance after structure modification, we obtained enough excellent derivatives for challenging the solubility and hERG inhibitory activity. On one hand, eighteen derivatives, inhibitory potency at the single-digit nanomolar level, were selected to explore the water solubility. As shown in Table 4, in general, compared with benzocycloalkane compounds, *chroman* and *coumaran* derivatives exhibited better solubility. New derivatives with the same substitutents as previous reported compounds (Figure S5) significantly increased the solubility,[31] at least ~ 10 folds elevated more than **4**, **5** and their analogs (**20**, **21**, **24** *vs* **4**, **4a**, **4b** *vs* **5**, **5a**, **5b**), whereas there was no significant difference between *chroman* and *coumaran* derivatives (**17** *vs* **55**, **23** *vs* **61**, **24** *vs* **62**, **31** *vs* **69** and **45** *vs* **83**), and these results further demonstrated the feasibility of scaffold hopping. However, it must be mentioned that the hydrophilic property of substitutents at the phenyl ring also affected the solubility of compounds. Compared with the derivatives with hydrophilic

substitutents, derivatives with lipophilic substitutents (**17**, **22**, **31**, **55** and **69**) restricted the solubility (all less than 7 mg/mL). On the other hand, fifteen compounds (pigment inhibition: $IC_{50} \leq 6$ nM) were screened for investigating the hERG inhibition. As opposed to the benefits of hydrophilic substitutents on solubility, they disclosed passive influence in regard to hERG inhibition, while lipophilic substitutents exhibited positive effects. As shown in Table 4, obviously, derivatives **17**, **55**, **31**, **69** and **30** (hERG inhibition, $IC_{50} > 6$ μM in whole) with lipophilic substitutents exhibited superior than the other ones (hERG inhibition, $IC_{50} < 4$ μM in whole). Even so, different from the elevation of solubility by means of many mature methods, the methods about decreasing hERG inhibition were currently occupied by chemical modification, which forced us to give priority to derivatives with weaker hERG inhibition for further explorations. Moreover, we had suggested that the problematic solubility could be resolved adequately by combining structural modification with salt type selection, and salt type selection as the other strategy was established and discussed below. Therefore, **31** and **69** were selected to further investigate due to their potent pigment inhibitory activity ($IC_{50} < 4$ nM), weak hERG inhibition ($IC_{50} > 10$ μM) and fair water solubility (Table 4). More coincidence, both of them contained para-biphenyl in their respective scaffolds, so we aimed to identify other potent inhibitors easier.

Table 1, Table 4

Analysis of the data in Table 2 revealed that once the *N*-methyl group was removed (**89, 90**) or converted into an ethyl or isopropyl group (**91-94**), the pigment

inhibition activities abated (IC_{50} > 1000 nM). As shown in Table 3, when the vinyl linker was replaced with a butadienyl, derivative **105** (IC_{50} = 3.0 ± 0.4 nM) evenly displayed the most potency in the other scaffold. Fortunately, the hERG inhibition IC_{50} value of **105** was greater than 40 μM, which was better than that of **31** (hERG inhibition IC_{50} = 32.1 μM, Table 4). All results showed that **105** was more eligible as the candidate compound. Elimination of the double bonds (**101**, **104**, **106** and **109**) led to a loss of pigment inhibitory activities (IC_{50} > 1000 nM). Subsequently, the introduction of an additional methyl moiety deprived the activities of derivatives (**102**, **107**, IC_{50} > 1000 nM). Finally, the introduction of a branched methyl on a vinyl linker resulted in a decrease in pigment inhibitory activity (IC_{50} = 17.3 ± 0.2 nM by **103** and IC_{50} = 23.5 ± 0.8 nM by **108**).

Tables 2-3

Structure-Activity, -Solubility and -hERG Inhibition Relationship

On the basis of the structural features and pigment inhibitory activities data, the SARs are summarized in detail. (1) According to the modification of region A, the potency improved obviously in the substituted phenyl >> heterocyclic = cycloalkyl. Regarding the substituted phenyl, the electronic effect of the substituent was limited to the pigment inhibitory activity, whereas the substituted position was fatal; notably, the para-position was the best substituted position at the phenyl ring. The suitable size of the substituent also affected the potency obviously. On the basis of these obtained results and hERG inhibition, the para-biphenyl substituents represented more potency than the others. (2) In the studied set replacing the N-methyl group with various steric

alkyl groups (hydrogen, ethyl and isopropyl), the size of the substituted group was crucial to the potency, and the N-methyl group was necessary for pigment inhibitory activities. (3) Multiallyl derivatives were synthesized by inserting one vinyl, and all of the derivatives showed excellent inhibitory activities, whereas other modifications showed that the unsubstituted allyl linker was critical for achieving high potency. (4) Based on the results of solubility and hERG inhibition, we found that the strategy of inserting hydrophilic oxygen into scaffolds remarkably increased the solubility of derivatives by comparing with the previous compounds, whereas lipophilic substituents at the phenyl ring weakened the efficiency but forcibly reduced hERG inhibitory activity.

Target CrtN Determination of Chroman and Coumaran Derivatives.

Benzocycloalkane derivatives were determined to be CrtN inhibitors in our previous research.[31] To confirm whether the target enzyme was the same as *coumaran* and *chroman* derivatives, we conducted identical HPLC experiments at 286 nm for the analysis of 4,4'-diapophytoene (the product of CrtM and the substrate of CrtN). As seen in Figure 3B, both the retention time and UV absorption spectra of 4,4′-diapophytoene were measured by monitoring the HPLC expression of CrtM in *E. coli*, which was found in the similar HPLC expression of wild-type *S. aureus* Newman (Figure 3C). Moreover, this HPLC peak disappeared in the carotenoid extracts of the CrtM mutant (Figure 3D) and was strengthened in the CrtN mutant (Figure 3E). It was reassuring to note that this peak belonged to 4,4'-diapophytoene. Comparing the HPLC peaks of **69** and **105**-treated wild-type *S. aureus* Newman

(Figure 3G-H) with NTF-treated Newman (Figure 3F), these profiles were not only identical to each other, but they were also similar to those of CrtM in *E. Coli* and the CrtM mutant. Consequently, all of the results demonstrated that CrtN was the target of *coumaran* and *chroman* derivatives **69** and **105**.

Figure 3

***In Vitro* Enzymatic and Pigment Inhibitory Activities of Four Representative Derivatives**

***In Vitro* CrtN Enzymatic Inhibitory Activities.** According to previous protocol,[29] selected derivatives in Table 5 (**31**, **62**, **69** and **105**) with pigment inhibitory activities IC_{50} < 4 nM in *S. aureus* Newman were evaluated for enzymatic inhibitory activities *in vitro*. The results showed that four derivatives displayed excellent enzymatic inhibitory activity of CrtN at submicromolar concentrations, though the enzymatic activities were less effective than pigment inhibition due to the accumulation of compounds in the cytoplasm of *S. aureus* and three sequential reactions using CrtN in the biosynthesis of STX, as we speculated in our previous papers.[29-31] In particular, derivatives **69** (IC_{50} = 181.3 ± 34.3 nM) and **105** (IC_{50} = 179.6 ± 29.5 nM) were superior than **4** (IC_{50} = 320 nM).

***In Vitro* Pigment Inhibitory Activities against MRSA.** Next, two community acquired MRSAs, USA400 MW2 and USA300 LAC,[37-38] along with other four hospital-acquired MRSAs, Mu50 (vancomycin-intermediate resistance, VISA/MRSA), and NRS271 (linezolid-resistance, LRSA/MRSA),[39-40] were used to demonstrate the broad spectra efficiency of derivatives **31**, **62**, **69** and **105**. Pigment inhibition results

of these MRSA strains are shown in Table 5**,** in which derivative either **69** or **105** showed better inhibitory activities in Mu50 (IC_{50} = 0.33 ± 0.3 nM, IC_{50} = 0.36 ± 0.1 nM, respectively) and NRS271 (IC_{50} = 1.7 ± 0.2 nM, IC_{50} =0.4±0.1 nM, respectively) in their respective series. For demonstrating the broad spectrum of **69** and **105**, NF65Y (vancomycin-intermediate resistance, VISA/MRSA) and LRSA56 (linezolid-resistance, LRSA/MRSA) were introduced into the assay, the results showed that two compounds displayed excellent potency. In contrast to the antibiotic, incubation with derivatives **69** or **105** did not affect the growth of *S. aureus* strains (Newman strain and three MRSA strains) at 0.2 mM. (Figure S1, *Supporting Information*).

Table 5

Effects of 69 and 105 on Sensitizing *S. aureus* to Immune Clearance.

Hydrogen Peroxide Killing Assay. Having confirmed that derivatives **69** and **105** displayed excellent potency *in vitro*, we then evaluated their effects on sensitizing *S. aureus* and three other MRSA strains (USA400 MW2, USA300 LAC, and Mu50) with pigment or non-pigmented for immune clearance as in the previous report, including the protocol of hydrogen peroxide killing and human whole blood killing.[29] As shown in Figure 4, after incubation with derivatives **69** or **105** (1 μM, respectively), non-pigmented *S. aureus* cells were more vulnerable to be killed by 1.5% H_2O_2, compared with the untreated *S. aureus* (mock) (survival rate, 2.6% vs 3.3% vs 33.3%). In parallel, the survival rate of the known antioxidant *N*-acetylcysteine (NAC)-treated *S. aureus* cells were more elevated than the mock, as expected (60.7% vs 33.3%).

Similarly, the survival percentages of the three MRSA strains were reduced by factors of ~ 10 (2.3% vs 24.3% by **69**, 2.6% vs 24.3% by **105**, in Mu50), ~ 10 (2.0% vs 24.0% by **69**, 2.3% vs 24.0% by **105**, in USA300 LAC), and ~10 (2.6% vs 26.3% by **69**, 2.5% vs 26.3% by **105**, in USA400 MW2), respectively. The survival rates of the three NAC-treated MRSA strains tended to be higher (50.7% vs 24.3% in Mu50, 54.7% vs 24.0% in USA300 LAC, 57.0% vs 26.3% in USA400 MW2). All of the results above proved that the addition of H_2O_2 (with strong oxidation) exerted impacts on the MRSA strain survival and the pigment definitely acted as a protective antioxidant.

Human Whole Blood Killing Assay against *S. aureus*. Firstly, incubating time and bacterial survival relationship was explored owing to the reproduce ability difference of strains in different time stages. Five time intervals were established throughout the assay, and associated with two hours in each interval. The results manifested that the bacterial survival of **69** or **105** treatment groups were lowest during the third interval (Figure S2, *Supporting Information*). On the basis of these results we defined six hours as the standard incubating time in whole blood killing assay. Subsequently, the other experiment was performed to compare the effects of compound-treated *S. aureus* with non-treated bacteria by human whole blood killing, as in previous research. As shown in Figure 5, the survival rates of the untreated *S. aureus* Newman and the other three MRSA strains were much higher, compared to the compound-treated ones (**69**, **105** and mock in order, 0.28% *vs* 0.63% *vs* 8.67% in

Newman, 0.46% *vs* 0.45% *vs* 9.33% in Mu50, 0.12% *vs* 0.23% *vs* 12.0% in USA300 LAC, and 0.20% *vs* 0.53% *vs* 20.67% in USA400 MW2).

Meanwhile, CrtN mutant *S. aureus* (depigment *S. aureus*) was introduced to incubate with/without our compounds in human blood, for determining whether our compounds stimulated mammalian immune response or not. This assay was made up of six groups, non-treated Newman, non-treated CrtN mutant *S. aureus*, **69**-treated Newman, **69**-treated CrtN mutant *S. aureus*, **105**-treated Newman and **105**-treated CrtN mutant *S. aureus*. As shown in Figure S3 in *Supporting Information*, although the non-treated CrtN mutant *S. aureus* group represented more potency compared with non-treated Newman (survival rate, 0.9% *vs* 9.3%) in whole blood killing, its efficiency had no significant difference with **69**/**105**-treated Newman (0.9% *vs* 1.1% *vs* 0.8%), and testified that non-pigment *S. aureus* itself was actually vulnerable to immune clearance. Similarly, compared with non-treated CrtN mutant *S. aureus* group, there were no more effects exhibited by **69**/**105**-treated groups against CrtN mutant *S. aureus* (0.9% *vs* 0.76% *vs* 0.93%), which demonstrated the efficiency of inhibiting unpigmented *S. aureus* failed to be strengthened with/without the treatment of our compounds. Furthermore, we suggested that compounds **69**/**105** had no effect on the stimulation of mammalian immune response in human blood killing assay. Consequently, all above results were indicated that derivatives **69** and **105** exclusively sensitized *S. aureus* to immune clearance in human blood.

Figures 4-5

***In Vivo* Pigment Inhibitory Activities of Derivatives 69 and 105**

Derivatives **69** and **105** had inspiring activities *in vitro*, and to test their potential pigment inhibitory activities *in vivo*, mice were challenged with 3.5×10^7 CFU Newman bacteria to evaluate the efficiencies of **69** and **105** on affecting the outcome of *S. aureus* (Figure S4*, Supporting Information*). The untreated group died out within 3 days, whereas **69** and **105** exhibited the excellent protective efficiencies, resulting in 73% and 67% animal survival respectively. As time went on to the sixth day, over 60% of the compound-treated mice were alive. These initial investigations clearly proved that the *in vivo* **69** and **105** treatment weakened the virulence of *S. aureus* Newman.

Next, four different drug regimens were applied, first two different doses, both 0.4 mg/bid/4.5 d (20 mg/kg/dose, 180 mg/kg in total dose) and 0.1 mg/bid/4.5 d (5 mg/kg/dose, 45 mg/kg in total dose) with pretreatment (pre-administration with drugs or derivatives 24 hours in advance before the infection of *S. aureus* strains) were set in previous works.[30-31] Then, both 0.4 mg/bid/3.5d (20 mg/kg/dose, 140 mg/kg in total dose) and 0.1 mg/bid/3.5d (5 mg/kg/dose, 35 mg/kg in total dose) with normal treatment (administered 6 hours after the infection of *S. aureus* strains) were set to simulate the real situation of infection and treatment. Linezolid (LZD) and vancomycin (VAN) were used for two positive controls at a dosage of 0.4 mg/bid/4.5d (20 mg/kg/dose, 180 mg/kg in total dose) with pretreatment.

***In Vivo* Effects of Derivatives 69 and 105 on Attenuating the Virulence of *S. aureus* Newman.** After infection with 2.3×10^7 colony-forming units (CFU) of *S. aureus* Newman bacteria via retro-orbital injection, the mice were sacrificed at ~108h.

We then measured bacterial survival in the hearts and livers. As shown in Figure 6A, in general, each case showed a significant reduction ($P < 0.001$ and more than a 95% decrease in surviving bacteria), compared to non-treatment group (6.18 $\log_{10}$ CFU) in hearts. In addition, **69** in the low-dosage case (5 mg/kg/dose) in normal treatment exhibited the same protective effects as the two positive cases with at high dosages (20 mg/kg/dose) in pretreatment (4.58 $\log_{10}$ CFU by **69** vs 4.62 $\log_{10}$ CFU by vancomycin vs 4.186 $\log_{10}$ CFU by linezolid). As shown in Figure 6B, firstly, compared with the non-treatment group (6.65 $\log_{10}$ CFU), the staphylococcal loads of all of the compound-treated groups were decreased in the livers with statistical significance ($P < 0.001$, except **105** treatment in 20 mg/kg/dose). The activities of **69** treatment groups were comparable to these in the **105** treatment groups. Apart from being inconsistent with the relationship of the dosage-activity (0.4 mg/bid vs 0.1 mg/bid), there was no significant difference between pre-administration and normal administration of **69** or **105** in the respective groups. In addition, the bacterial survival rates of the high-dosage cases were slightly elevated relative to the two positive groups, and they demonstrated a comparative clearance (all group significance $P > 0.05$). To our surprise, both **69** treatment and **105** treatment with low dosages in the normal group (5 mg/kg/dose, 2.12 $\log_{10}$ CFU reduction by **69** treatment, 1.80 $\log_{10}$ CFU reduction by **105** treatment, respectively) had a more than 98% decrease in surviving bacteria, especially the **69** treatment, which showed a 99.3% decrease in surviving bacteria, comparable to the LZD-treatment group (1.74 $\log_{10}$ CFU reduction, a 98.2% decrease in surviving bacteria) and the VAN-treatment group (1.77 $\log_{10}$ CFU

reduction, a 98.3% decrease in surviving bacteria). These results demonstrated clearly that *in vivo* **69** treatment excellently attenuated the pathogenicity of *S. aureus* Newman in contrast to the positive groups, especially the effects of **69** treatment at low-dosages in the normal treatment group. Moreover, the lack of significant difference between the pre-administration and normal administration groups indicated that our derivatives were closer to practical application.

Figure 6

***In Vivo* Effects of Derivatives 69 and 105 on Attenuating the Virulence of Mu50 MRSA.** Next, to determine whether the effects of derivatives **69** and **105** could also be reflected in multi-drug resistant MRSA strains *in vivo*, a vancomycin-intermediate *S.aureus* (VISA, Table S3, *Supporting Information*), Mu50 infection model was established. The data in Figure **7A** revealed that derivative-treatment groups significantly decreased Mu50 staphylococcal loads in the hearts. All of them corresponded to a more over 95.0% decrease in surviving bacteria (significance $P < 0.001$), while the derivative-treatment groups were also more efficacious than the two positive groups, VAN and LZD, by 0.96 and 1.07 $\log_{10}$ CFU, corresponding to 89.1% and 91.5% decreases, respectively. In general, all of the regimens with **69** represented excellent potency without significant differences, whereas enormous differences were shown between the pre-administration and normal administration cases in the **105** treatment groups. Obviously, **69** and **105** treatment with low dosages in normal administration groups displayed better activity among the respective groups again (2.39 $\log_{10}$ CFU reduction by **69** treatment, 2.32 $\log_{10}$ CFU reduction by **105**

treatment, more than 99.0% decrease in surviving bacteria, respectively). As shown in Figure **7B**, compared with the non-treatment group, the effects of attenuating the virulence of Mu50 MRSA in the livers of the derivatives-treatment group indicated more potency (all groups' significance $P < 0.001$, more than a 98% decrease in surviving bacteria), whereas the two positive groups performed better than most of the derivatives-treatment groups (2.75 $\log_{10}$ CFU reduction by VAN treatment and 3.19 $\log_{10}$ CFU reduction by LZD treatment, corresponding to 99.8% and 99.9% decreases, respectively.). The therapeutic efficiency between **69** treatment at low-dosage in normal treatment by 3.15 $\log_{10}$ CFU and the two positive groups were at comparable levels, with a remarkable ~99.9% decrease in surviving bacteria.

Figure 7

***In Vivo* Effects of Derivatives 69 and 105 on Attenuating the Virulence of NRS271 MRSA.** To assess the spectrum of activities of **69** and **105**, we evaluated their antibacterial activity against NRS271 strains *in vivo* (linezolid-resistant *S.aureus*, LRSA, Table S3, *Supporting Information*). As shown in Figure **8A**, although the value of the LZD group was superior to the non-treatment group (significance $P < 0.001$ reduction, a 91.7% decrease in surviving bacteria), it still displayed weak inhibitory activity, compared with the other groups in the experiment. In contrast to the LZD-treatment group treated with NRS271, the derivative-treatment groups always exhibited significant effects in comparison with non-treatment group in hearts (all compound-treatment group significance $P < 0.001$, over 93% decrease in surviving bacteria). In addition, either **69** or **105** in the low-dosage case represented more

efficacious results (significance difference with the LZD-treatment group $P < 0.01$, ~ 2.4 $\log_{10}$ CFU reduction, a remarkable ~ 99.5% decrease in surviving bacteria, respectively), and they were not only at comparative levels to the VAN-treatment group (2.6 $\log_{10}$ CFU reduction, a ~99.8% decrease in surviving bacteria), but they also had greater potency than the other groups. As shown in Figure **8B**, similar to the effects in hearts, the strains were weakened continuously in the LZD-treatment group in livers. However, our treatment groups still showed excellent performance. In particular, four **105**-treatment groups significantly decreased their NRS271 staphylococcal loads in the livers by 2.13 $\log_{10}$ CFU at least (more than a 99.3% decrease in surviving bacteria), whereas the LZD-treatment group led to a reduction by only 1.19 $\log_{10}$ CFU, making it less efficacious than **105** treatment. In particular, the bacterial survival rates of **105** treatment in low-dosage cases demonstrated comparative clearance to the VAN-treatment group, while the **69**-treatment groups maintained a comparative level with LZD treatment and a worse level than the VAN-treatment groups.

In summary, two STX biosynthesis inhibitors, either **69** or **105**, was capable of decreasing the bacterial survival in the abscess formation model of *S. aureus* Newman, MRSA and LRSA strains. Moreover, some of the **69** or **105** treatment groups were more efficacious than the two positive groups, especially **69** treatment with a low dosage in normal treatment. Furthermore, derivative **69** was slightly more successful than **105** in comparing the two under the same conditions. In addition, the experiment demonstrated that there was no significant difference between the pretreatment

regimens with normal treatment. To our surprise, the low-dosage groups had excellent performance, compared with the high-dosage cases in general. The speculated reasons are provided as follows: (1) according to the pigment inhibitory activity of derivative (IC_{50} < 4 nM), the high dosage was more than sufficient for its purpose; and (2) high dosages possibly weakened the ability of immune clearance *in vivo*, which destabilized the situations of dosage and activity.

Figure 8

***In Vivo* Rat Pharmacokinetics Parameters of 69**

Since its potency and therapeutic profiles, candidate **69** as the representative was evaluated to rat pharmacokinetic (PK) *in vivo*. The pharmacokinetic parameters were administrated with either IV injection of a single 5mg/kg dose or PO administration of a single 10 mg/kg dose. As a result, candidate **69** exhibited fair pharmacokinetic properties (F = ~7%) after oral administration of a 10 mg/kg dose to rats, and its pharmacokinetic data are summarized in Table 6. Additionally, pharmacokinetic analysis about injectable administration revealed that **69** had a C_{max} of 2044ng/mL and $t_{1/2}$ of 2.3 h.

Table 6

***In Vitro* Antifungal Activities of 69 and 105**

Because **69** and **105** was derived from mother nucleus structure of **2**, a drug used in antifungals, it was rational to investigate whether our derivatives inherited the antifungal activity. As shown in Table 7, three fungus strains and three first-line drugs were chosen to proceed with the *in vitro* assay. Compared with the three positive

groups, **69** and **105** exhibited weak activities against all three dermatophytes. This result partly demonstrated our derivatives to be promising selective antibacterial candidates.

Table 7

Salt Type Selection

Although overall solubility of *chroman* and *coumaran* derivatives significantly increased by inserting a hydrophilic oxygen into the cycloalkane, the optimized candidates **69** (4.4 mg/mL) and **105** (3.8 mg/mL) still were not more soluble than benzocycloalkane **4**. Herein, salt type selection was set up for eliminating this flaw. As shown in Table 8, ten different acids were introduced to salify with either **69** or **105** free base. Notably, phosphate **69b** and **105b** represented remarkable improvement of solubility (16.2 mg/mL and 12.9 mg/mL, respectively).

Table 8

Conclusion

In this study, two series of derivatives (*chroman* and *coumaran*), ninety-two in total, were synthesized, and we evaluated their activity against wild-type *S. aureus* Newman and several MRSA strains systematically. According to the results of the pigment inhibitory activities against *S. aureus* Newman, unambiguous SARs were obtained. Four derivatives (**31**, **62**, **69** and **105**) were selected and subjected to further evaluation of their outstanding pigment inhibitory activities. Finally, derivatives **69** and **105** were carefully selected from respective series since they exhibited favorable characteristics *in vitro*, including hERG activities (IC_{50} = 11.3 μM and IC_{50} > 40 μM,

respectively), enzymatic activities and pigment inhibitory activities of six other MRSA strains. The experiments of bacterial growth assays and immune clearance proved that **69** and **105** could sensitize *S. aureus* strains to be killed by H_2O_2 or human blood, neither interfering the bacterial growth nor stimulating mammalian immune response. Derivatives **69** and **105** also displayed a broad and significantly potent antibacterial spectrum *in vivo* against pigmented *S. aureus* Newman, Mu50 (VISA/MRSA) and NRS271 (LRSA/MRSA). By means of the four different drug regimens established, **69** treatment with low-dosages in the normal treatment group (5 mg/kg/dose, 35 mg/kg in total dose) showed comparable effects to the two positive groups (linezolid and vancomycin) in the liver in Newman and Mu50 and they even more effective than in the two positive groups in the heart in Mu50, whereas **105** treatment with low-dosage cases (5 mg/kg/dose) possessed excellent inhibitory activities compared to vancomycin in the hearts and livers in NRS271. Additionally, **69** and **105** exhibited weak activities against fungals, and **69** exhibited the average pharmacokinetic efficiency. Furthermore, phosphate **69b** and **105b** disclosed remarkable solubility by salt type selection. The favorable *in vitro* and in *vivo* activities of **69** and **105**, combined with their superior solubility and hERG safety profiles, made them promising drug candidates. Further evaluation of these two drug candidates is currently under way.

EXPERIMENTAL SECTION

General Chemistry

Reagents and solvents were obtained from commercial suppliers at high quality and were used without further purification. TLC was performed on a HSGF 254 (150-200 μm thickness; Yantai Huiyou Co., China). UV light and I_2 were used to monitor synthetic progress. Column chromatography was performed on silica gel (200-300 mesh), eluted with ethyl acetate and petroleum ether. NMR spectra data were obtained on a Bruker AMX-400 NMR using TMS as an internal standard. Chemical shifts were provided in parts per million. ^{1}H NMR data were reported from the aspect of multiplicity (s = singlet, d = doublet, t = triplet, q = quartet, m = multiplet and br = broad), coupling constant (Hz) and integrated value. Low- and high-resolution mass spectral (MS) data were acquired with electron spray ionization (ESI) produced by a Finnigan MAT-95 and LCQ-DECA spectrometer. The purity of each compound (> 95%) was determined by HPLC on an Agilent 1100 with a quaternary pump and diode-array detector (DAD). The melting points of each compound were determined on an SGW X-4 melting point apparatus.

General Procedure A for Preparation of Salts.

Taking **69** free base as an example, to a solution of oily derivative **69** free base (100 mg) in ethyl ether (10 mL) stirred at room temperature with hydrochloride gas or 1.1 equivalent of other acids for 1 min. After stirring for 15 min, the solvent was removed by rotary evaporation and the residue was suspended in ethyl acetate/petroleum ether (1:100, v/v, 10 mL) for an additional hour of agitation. The precipitate was filtrated and washed with petroleum ether to obtain the final compound in the form of hydrochloride or other acids. All other final derivatives

underwent through this process to yield an amorphous, solid form or oil. Spectroscopic data reported below are in their hydrochloride form (*Supporting Information*).

General Procedure B for Preparation of Salts.

To a solution of **69** or **105** (10 mmol) in EtOAc was treated with the solution of acid (10 mmol) in EtOH in batches at room temperature, the mixture was then allowed to stir at 80 ºC for an additional 1 hour, the solvent was removed by rotary evaporation and the residue was suspended in ether for an additional hour of agitation. The precipitate was filtrated and washed with ether to obtain the final salt, respectively.

Biological

Pigment Inhibition Assay. Newman bacteria were cultured in TSB (4 mL) medium at 37 ºC for 48 h with inhibitor compounds dissolved in DMSO and diluted to a set of concentrations, in duplicate. Three milliliters of bacterial cultures were centrifuged and washed twice with 0.01 M phosphate-buffered saline (PBS) and resuspended in methanol to extract pigment. The absorbance value was determined at 450 nm on a NanoDrop 2000c (Thermo Scientific) spectrophotometer. IC_{50} values were calculated using Graphpad Prism software, version 5.0. The IC_{50} values of the USA300 LAC, USA400 MW, Mu50, NRS271, NF65Y and LRSA56 strains were determined in the same manner.

CrtN Enzyme Inhibition Assay. Diapophytoene was purified from diapophytoene-producing *E. coli* BL21 (DE3) /pET28a :: *crtM* extracted with acetone.

Eight milligrams of diapophytoene were mixed with 24 mg of phosphatidylcholine (Sigma-Aldrich) in 200 μL of $CHCl_3$ to prepare the diapophytoene emulsion. The mixture was spin-dried and incubated with 2 mL of 0.02 M HEPES buffer (pH = 7.5) followed by sonication in ice water to obtain the homogeneous emulsion. For the preparation of CrtN lysate, *E. coli* BL21 (DE3)/pET28a :: *crtN* was sub-cultured into 1000 mL of LB broth supplemented with 50 μg/mL kanamycin to achieve an OD_{600} (Eppendorf, BioPhotometer plu) of ~ 0.1 and was grown to an OD_{600} of ~ 0.5. The expression of 6His-CrtN protein was induced with 0.5 mM isopropyl-*β*-D-thiogalactoside (IPTG) at 16 °C overnight. The cells were harvested, and the pellets were suspended in 30 mL HEPES buffer and lysed at 4 °C by sonication.

The enzyme activity was determined in triplicate, with a total of 700 μL of the following: 50 μL of diapophytoene emulsion, 70 μL of different concentrations of compounds or mock (ddH_2O), 3.5 μL of FAD stock solution (10 mM), and 300 μL of CrtN lysate (~1.41 mg of CrtN, as estimated by western blotting using a known concentration of the purified 6His-crtN protein), followed by 0.02 M HEPES buffer (pH 7.5) to 700 μL. The tests were proceeded in an anaerobic atmosphere by adding a final concentration of 20 U/mL glucose oxidase (Sigma-Aldrich, G2133), 20000 U/mL catalase (Sigma-Aldrich, C1345), and 2 mM glucose as an oxygen-trapping system. The reaction mixture was started by adding the lysate and incubating it overnight at 37 ºC and then stopped by methanol. The pigments were extracted twice against 700 μL of chloroform. The organic phase was combined, concentrated, and

redissolved in 200 μL of chloroform and $OD_{450}$was recorded. The IC_{50} values were obtained by fitting the OD data to a normal dose-response curve using Graphpad Prism 5.0 software.

Hydrogen Peroxide Killing and Human Whole Blood Killing. For H_2O_2 killing assay, four strains, including Newman, USA300 LAC, USA400 WM2 and Mu50, were cultured in TSB and grown at 37 °C for 24 h with or without 1 μM derivative **69** or **105** or *N*-acetylcysteine (NAC). The bacteria were washed twice in PBS and then were diluted to a concentration of 4×10^6 CFU per 250 μL reaction mixture in a 1 mL Eppendorf tube. After H_2O_2 was added to a final concentration of 1.5%, the tubes were incubated for 30 min at 37 ºC with shaking at 250 r.p.m. The reaction was terminated by the addition of 1000 U/mL exogenous catalase (Sigma-Aldrich). Bacterial survival was assessed by serial dilutions on TSA and TSB plates in parallel for the enumeration of CFUs.

For human whole blood killing assay, overnight cultured strains were centrifuged and suspended in sterile PBS to generate a suspension of 1×10^7 CFU/mL. Whole blood (360 μL) from healthy human volunteers was collected using a BD VACUTAINER PT tube and then was mixed with 40 μL bacterial samples, resulting in a concentration of 1×10^6 CFU/mL. The tubes were incubated at 37 ºC for 6 h, and then the dilutions were plated on TSA agar and TSB plates in parallel for enumeration of the surviving CFUs.

***S. aureus* Systemic Infection Models.** Six- to 8-week-old female BALB/c mice (20 g weighed) were obtained from JSJ Lab Animal, Ltd. and were housed under specified

pathogen-free conditions. Seven groups (pretreatment), including four groups of **69** or **105** at two different doses (45 mg/kg and 180 mg/kg), two groups of vancomycin or linezolid at a dose of 180 mg/kg and the mock group, at 12 h intervals for 108 hours (4.5 d), were infected by retro-orbital injection with a suspension of staphylococci 12 hours after the first intraperitoneal injection, while the other four groups (normal treatment), including **69** or **105** at two different doses (35 mg/kg or 140 mg/kg), in 12 intervals for 84 hours (3.5 d), had the first administration given to mice 6 hours after challenge with *S.aureus* strains. All the compounds were dissolved in sterile ddH_2O plus 10% castor oil ethoxylated. For the mouse model of abscess formation, the mice were challenged with 100 μL of a bacterial suspension of 2.3×10^7 CFU of *S. aureus* Newman, 1.1×10^9 CFU of *S. aureus* Mu50, or 1.9×10^8 CFU of *S. aureus* NRS271. Animals were sacrificed ~84 hours after infection. The hearts and livers were aseptically removed and homogenized in 1 mL of PBS plus 0.01% Triton X-100 to obtain single-cell suspensions, and serial dilutions of each organ were plated on TSA agar and TSB plates in parallel for the enumeration of CFUs by an operator blind to treatment. The statistical significance was determined by the Mann-Whitney test (two-tailed).

Anti-fungal Assays. *In vitro* antifungal activity was determined by measuring the minimal inhibitory concentrations using the broth microdilution recommended by the National Committee for Clinical Laboratory Standards (NCCLS). *Microsporum gypseum*, *Trichophyton rubrum* and *Tinea barbae* as common pathogenic fungi were selected as the tested fugal strains and were incubated with serially diluted test

compounds in 96-well microtest plates at 28 °C for 7 days. The MIC value was defined as the lowest concentration of a test compound that resulted in a culture with turbidity less than or equal to 80% inhibition, compared to the growth of the control.

***In Vivo* Pharmacokinetics Analysis**. The pharmacokinetic properties of **69** were analyzed by the Medicilon Company, Shanghai, China. Six male SD rats (230-260 g weighed) were purchased from Shanghai SIPPR-BK LAB Animal Ltd., Shanghai, China, and used for the pharmacokinetic analysis of **69**. **69** was dissolved in 10% castor oil/water for intravenous administration (IV) and oral administration (PO). A final dosage of 5 and 10 mg/kg of compounds was administered for IV and PO purposes, respectively, and the blood samples were taken at various time points during a 24 h period. The concentration of the compounds in the blood was analyzed by LC-MS/MS.

ASSOCIATED CONTENT

Supporting Information.

HPLC analysis data of derivatives **11-86**, **89-94** and **100-109**, experimental procedures and characterizations of derivatives, bacterial growth assays of *S. aureus* Newman and MRSA strains, the hERG inhibition assay and MIC values of derivatives against MRSA strains: This material is available free of charge via the Internet at http://pubs.acs.org.

AUTHOR INFORMATION

Corresponding Author

*For J.L.: Phone, +86-21-64252584; Fax, +86-21-64252584; E-mail: jianli@ecust.edu.cn; For L.L.: Phone, +86-21-50803109; E-mail: llan@simm.ac.cn.

Author Contributions

†These authors contributed equally to this work.

Notes

The authors declare no competing financial interests.

ACKNOWLEDGMENTS

Financial support for this research provided by the National Natural Science Foundation of China (Grant 21672064), the National Key R&D Program of China (Grant 2017YFB0202600), the "Shu Guang" project supported by the Shanghai Municipal Education Commission and Shanghai Education Development Foundation (Grant 14SG28), and the Fundamental Research Funds for the Central Universities are gratefully acknowledged.

ABBREVIATIONS

S. aureus, *Staphylococcus aureus*; MRSA, methicillin-resistant *Staphylococcus aureus*; STX, staphyloxanthin; NTF, naftifine hydrochloride; ND4BB, New Drugs for Bad Bugs; CrtM, dehydrosqualene synthase; CrtN, diapophytoene desaturases; ROS, reactive oxygen species; PK, pharmacokinetics; SAR, structure-activity relationship; IC_{50}, half maximal inhibitory concentration; MIC, minimum inhibitory concentration; HPLC, high-performance liquid chromatography; MS, mass chromatography; CFU, colony-forming unit; PBS, phosphate-buffered saline; DMF, *N,N*-dimethylformamide; DMSO, dimethyl sulfoxide; EtOH, ethanol; EtOAc, ethyl acetate; MeOH, methanol;

THF, tetrahydrofuran; CH_2Cl_2, dichloromethane; CH_3CN, acetonitrile; Et_3N, trimethylamine

REFERENCES

(1) Chambers, H. F.; Deleo, F. R. Waves of Resistance: *Staphylococcus aureus* in the Antibiotic Era. *Nat*. *Rev*. *Microbiol*. **2009**, *7*, 629-641.

(2) Zhan, C; Miller, M. R. Excess length of stay, charges, and mortality attributable to medical injuries during hospitalization. *JAMA* **2003**, *290*, 1868-1874.

(3) Graffunder, E. M.; Venezia, R. A. Risk factors associated with nosocomial methicillin-resistant *Staphylococcus aureus* (MRSA) infection including previous use of antimicrobials. *J*. *Antimicrob*. *Chemother*. **2002**, *49*, 999-1005.

(4) Grundmann, H.; Hori, S.; Winter, B.; Tami, A.; Austin, D. J. Risk factors for the transmission of methicillin-resistant *Staphylococcus aureus* in an adult intensive care unit: fitting a model to the data. *J*. *Infect*. *Dis*. **2002**, *185*, 481-488.

(5) Jevons, M. P. "Celbenin"- resistant Staphylococci. *Br*. *Med*. *J*. **1961**, *1*, 124-125.

(6) David, M. Z.; Glikman, D.; Crawford, S. E.; Peng, J.; King, K. J.; Hostetler, M. A.; Boyle-Vavra, S.; Daum, R. S. What is community-associated methicillin-resistant *Staphylococcus aureus*? *J*. *Infect*. *Dis*. **2008**, *197*, 1235-1243.

(7) Wulf, M.; Voss, A. MRSA in livestock animals-an epidemic waiting to happen? *Clin*. *Microbiol*. *Infect*. **2008**, *14*, 519-521.

(8) Van Cleef, B. A.; Monnet, D. L.; Voss, A.; Krziwanek, K.; Allerberger, F.; Struelens, M.; Zemlickova, H.; Skov, R. L.; Vuopio-Varkila, J.; Cuny, C.; Friedrich, A. W.; Spiliopoulou, I.; Paszti, J. ;Hardardottir, H.; Rossney, A.; Pan, A.; Pantosti, A.; Borg, M.; Grundmann, H.; Mueller-Premru, M.; Olsson-Liljequist, B.; Widmer, A.; Harbarth, S.; Schweiger, A.; Unal, S.; Kluytmans, J. A.

Livestock-associated methicillin-resistant *Staphylococcus aureus* in humans, Europe. *Emerging Infect*. *Dis*. **2011**, *17*, 502-505.

(9) Nicholson, T. L.; Shore, S. M.; Smith, T. C.; Frana, T. S. Livestock-associated Methicillin-Resistant *Staphylococcus aureus* (LA-MRSA) Isolates of Swine Origin form Robust Biofilms. *PLoS One* **2013**, *8*, e73376.

(10) Russoa, A.; Campanileb, F.; Falconea, M.; Tascinic, C.; Bassettid, M.; Goldonia, P.; Trancassinia, M.; Siegad, P. D.; Menichettic, F.; Stefanib, S.; Vendittia M. Linezolid-resistant staphylococcal bacteraemia: A multicentre case-case-control study in Italy. *Int*. *J*. *Antimicrob*. *Agents* **2015**, *45*,255-261.

(11) Rossi, F.; Diaz, L.; Wollam, A.; Panesso, D.; Zhou, Y.; Rincon, S.; Narechania, A.;Xing, G.; Di-Gioia, T. S.; Doi, A.; Tran, T. T.; Reyes, J.; Munita, J. M.; Carvajal , L. P.; Hernandez-Roldan, A.; Brandão, D.; van der Heijden, I. M.; Murray, B. E.; Planet, P. J.; Weinstock, G. M.; Arias, C. A. Transferable vancomycin resistance in a community-associated MRSA lineage. *N*. *Engl*. *J*. *Med*. **2014**, *370*, 1524-1531.

(12) Antibiotic Resistance: The Global Threat (U.S.); Centers for Disease Control and Prevention: Atlanta, GA, http://stacks.cdc.gov/view/cdc/31340 (accessed February 27, 2015).

(13) Global priority list of antibiotic-resistant bacteria to guide research, discovery, and development of new antibiotics; World Health Organization, http://www.who.Int/medicines/publications/WHO-PPL-Short_Summary_25Feb-ET_NM_WHO. pdf? ua =1 (accessed February 27, 2017).

(14) Medzhitov, R. Recognition of microorganisms and activation of the immune response. *Nature* **2007**, *449*, 819-826.

(15) Wang, R.; Braughton, K. R.; Kretschmer, D.; Bach, T. H.; Queck, S. Y.; Li, M.; Kennedy, A. D.; Dorward, D. W.; Klebanoff, S. J.; Peschel, A.; DeLeo, F. R.; Otto, M. Identification of novel cytolytic peptides as key virulence determinants for community-associated MRSA. *Nat. Med.* **2007**, *13*, 1510-1514.

(16) Escaich, S. Antivirulence as a new antibacterial approach for chemotherapy. *Curr. Opin. Chem. Biol.* **2008**, *12*, 400-408.

(17) Clauditz A.; Resch A.; Wieland K.P.; Peschel A.; Götz F.; Staphyloxanthin plays a role in the fitness of *Staphylococcus aureus* and its ability to cope with oxidative stress. *Infect. Immun.* **2006**, *74*, 4950-4953.

(18) Liu, G. Y.; Essex, A.; Buchanan, J. T.; Datta, V.; Hoffman, H. M.; Bastian, J. F.; Fierer, J.; Nizet, V. *Staphylococcus aureus* golden pigment impairs neutrophil killing and promotes virulence through its antioxidant activity. *J. Exp. Med.* **2005**, *202*, 209-215.

(19) Oldfield, E.; Feng, X. Resistance-resistant antibiotics. *Trends Pharmacol. Sci.* **2014**, *35*, 664-674.

(20) Raisig, A.; Sandmann, G. 4, 4'-diapophytoene desaturase: catalytic properties of an enzyme from the C (30) carotenoid pathway of *Staphylococcus aureus*. *J. Bacteriol.* **1999**, *181*, 6184-6187.

(21) Wieland, B.; Feil, C.; Gloria-Maercker, E.; Thumm, G.; Lechner, M.; Bravo, J. M.; Poralla, K.; Götz, F. Genetic and biochemical analyses of the biosynthesis of the

yellow carotenoid 4, 4'-diaponeurosporene of *Staphylococcus aureus*. *J. Bacteriol*. **1994**, *176*, 7719-7726.

(22) Hammond, R. K.; White, D. C. Inhibition of carotenoid hydroxylation in *Staphylococcus aureus* by mixed-function oxidase inhibitors. *J. Bacteriol*. **1970a**, *103*, 607-610.

(23) Hammond, R. K.; White, D. C. Inhibition of vitamin K2 and carotenoid synthesis in *Staphylococcus aureus* by diphenylamine. *J. Bacteriol*. **1970b**, *103*, 611-615.

(24) Kuroda, M.; Nagasaki, S.; Ohta, T. Sesquiterpene farnesol inhibits recycling of the C55 lipid carrier of the murein monomer precursor contributing to increased susceptibility to β-lactams in methicillin-resistant *Staphylococcus aureus*. *J. Antimicrob. Chemother*. **2007**, *59*, 425-432.

(25) Leejae, S.; Hasap, L.; Voravuthikunchai, S. P. Inhibition of staphyloxanthin biosynthesis in *Staphylococcus aureus* by rhodomyrtone, a novel antibiotic candidate. *J. Med. Microbiol*. **2013**, *62*, 421-428.

(26) Liu, C. I.; Liu, G. Y.; Song, Y.; Yin, F.; Hensler, M. E.; Jeng, W. Y.; Nizet, V.; Wang, A. H.; Oldfield, E. A cholesterol biosynthesis inhibitor blocks *Staphylococcus aureus* virulence. *Science* **2008**, *319*, 1391−1394.

(27) Song, Y.; Lin, F. Y.; Yin, F.; Hensler, M.; Rodrígues-Poveda, C. A.; Mukkamala, D.; Cao, R.; Wang, H.; Morita, C. T.; Gonzaleź-Pacanowska, D.; Nizet, V.; Oldfield, E. Phosphonosulfonates are potent, selective inhibitors of dehydrosqualene synthase and staphyloxanthin biosynthesis in *Staphylococcus aureus*. *J. Med. Chem*. **2009**, *52*, 976-988.

(28) Song, Y.; Liu, C. I.; Lin, F. Y.; No, J. H.; Hensler, M.; Liu, Y. L.; Jeng, W. Y.; Low, J.; Liu, G. Y.; Nizet, V.; Wang, A. H. J.; Oldfield, E. Inhibition of staphyloxanthin virulence factor biosynthesis in *Staphylococcus aureu*s: in vitro, in vivo, and crystallographic results. *J. Med. Chem.* **2009**, *52*, 3869-3880.

(29) Chen, F.; Di, H.; Wang, Y.; Cao, Q.; Xu, B.; Zhang, X.; Yang, N.; Liu, G.; Yang, C. G.; Xu, Y.; Jiang, H.; Lian, F.; Zhang, N.; Li, J.; Lan, L. Small molecule targeting of a diapophytoene desaturase inhibits *S. aureus* virulence. *Nat. Chem. Biol.* **2016**, *12*, 174-179.

(30) Wang, Y.; Chen, F.; Di, H.; Xu, Y.; Xiao, Q.; Wang, X.; Wei, H.; Lu,Y.; Zhang, L.; Zhu, J.; Sheng, C.; Lan, L.; Li. J. Discovery of Potent Benzofuran-Derived Diapophytoene Desaturase (CrtN) Inhibitors with Enhanced Oral Bioavailability for the Treatment of Methicillin-Resistant *Staphylococcus aureus* (MRSA) Infections. *J. Med. Chem.* **2016**, *59*, 3215-3230

(31) Wang, Y.; Di, H.; Chen, F.; Xu, Y.; Xiao, Q.; Wang, X.; Wei, H.; Lu, Y.; Zhang, L.; Zhu, J.; Lan, L.; Li. J. Discovery of Benzocycloalkane Derivatives Efficiently Blocking Bacterial Virulence for the Treatment of Methicillin-Resistant *S. aureus* (MRSA) Infections by Targeting Diapophytoene Desaturase (CrtN). *J. Med. Chem.* **2016**, *59*, 4831−4848.

(32) Müller, C. A.; Pfaltz, A. Mass spectrometric screening of chiral catalysts by monitoring the back reaction of quasienantiomeric products: palladium-catalyzed allylic substitution. *Angew. Chem.* **2008**, *47*, 3363-3366.

(33) THOMPSON; Wayne, J. Morphline Carboxamide prokineticin receptor antagonists. WO 2007067511, 2007.

(34) Kigawa, H.; Takamuku, S.; Toki, S.; Kimura, K.; Takeda, S.; Tsumori, K.; Sakurai, H. Intramolecular Electron Transfer and S_N2 Reactions in the Radical Anions of 1-(4-Biphenylyl)-ω-haloalkane Studied by Pulse Radiolysis. *J. Am. Chem. Soc.* **1981**, *103*, 5176-5179.

(35) Kawamata, Y.; Hashimoto, T.; Maruoka, K. A Chiral Electrophilic Selenium Catalyst for Highly Enantioselective Oxidative Cyclization. *J. Am. Chem. Soc.* **2016**, *138*, 5206–5209.

(36) Aldrich, C.; Bertozzi, C.; Georg, G. I.; Kiessling, L; Lindsley, C.; Liotta, D.; MerzJr., K. M..; Schepartz, A.; Wang, S. The Ecstasy and Agony of Assay Interference Compounds. *J. Med. Chem.* **2017**, *60*, 2165–2168

(37) David, M. Z.; Daum, R. S. Community-associated methicillin-resistant *Staphylococcus aureus*: epidemiology and clinical consequences of an emerging epidemic. *Clin. Microbiol. Rev.* **2010**, *23*, 616-687.

(38) de Matos P. D.; de Oliveira T. L.; Cavalcante F. S.; Ferreira D. C.; Iorio N. L.; Pereira E. M.; Chamon R. C.; Dos Santos K. R. Molecular markers of antimicrobial resistance in methicillin-resistant *Staphylococcus aureus* SCC*mec* IV presenting different genetic backgrounds. *Microb. Drug. Resist.* **2016**, April 5, doi:10.1089/mdr.2015.0255.

(39) Kuroda, M.; Ohta, T.; Uchiyama, I.; Baba, T.; Yuzawa, H.; Kobayashi, I.; Cui, L.; Oguchi, A.; Aoki, K.; Nagai, Y.; Lian, J.; Ito, T.; Kanamori, M.; Matsumaru, H.;

Maruyama, A.; Murakami, H.; Hosoyama, A.; Mizutani-Ui, Y.; Takahashi, N. K.; Sawano, T.; Inoue, R. i.; Kaito, C.; Sekimizu, K.; Hirakawa, H.; Kuhara, S.; Goto, S.; Yabuzaki, J.; Kanehisa, M.; Yamashita, A.; Oshima, K.; Furuya, K.; Yoshino, C.; Shiba, T.; Hattori, M.; Ogasawara, N.; Hayashi, H.; Hiramatsu, K. Whole genome sequencing of meticillin-resistant *Staphylococcus aureus*. *Lancet*. **2001**, *357*, 1225-1240.

(40) Wilson, P.; Andrews, J. A.; Charlesworth, R.; Walesby, R.; Singer, M.; Farrel, D. J.; Robbins, M. Linezolid resistance in clinical isolates of *Staphylococcus aureus.* *J. Antimicrob. Chemother*. **2003**, *51*, 186–188.

FIGURES

Figure 1. Structures of representative pigment inhibitors reported in the literature.

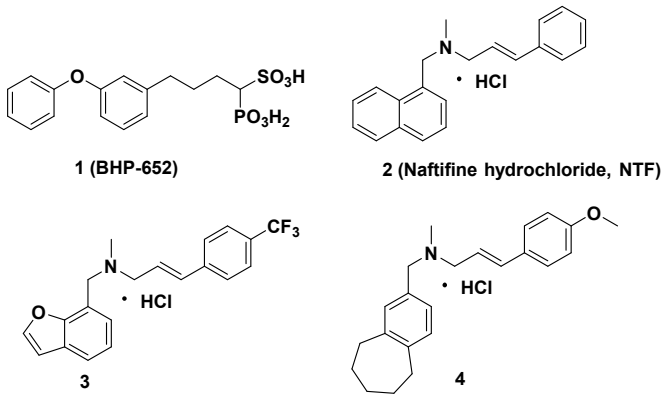

Figure 2. The structural evolution and two series (Series B and Series C) of compounds derived from lead compound **5**.

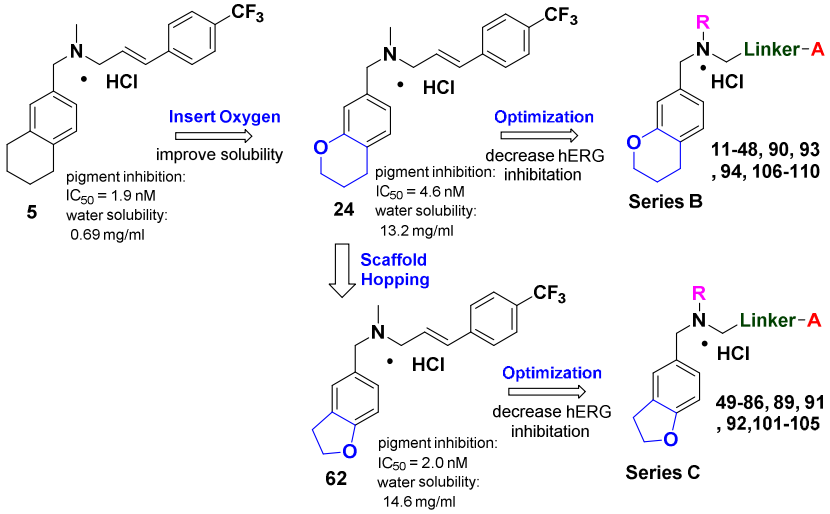

Figure 3. 69 and **105** treatment resulted in the inhibition of the *in vivo* function of CrtN. (A-H) HPLC chromatograms (absorption at 286 nm) of the carotenoid extracts from *E. coli* (A), *E. coli* expressing *S. aureus crtM* (B), wild-type *S. aureus* Newman (C), CrtM mutant (D), CrtN mutant (E), NTF-treated wild-type *S. aureus* Newman (F), **69**-treated wild-type *S. aureus* Newman strains (G), and **105**-treated wild-type *S. aureus* Newman strains (H). Insets on the right show the absorbance spectra of the indicated HPLC peaks. mAu, milli-absorbance units. Absorbance (Abs) represents the amount of light absorbed by the sample.

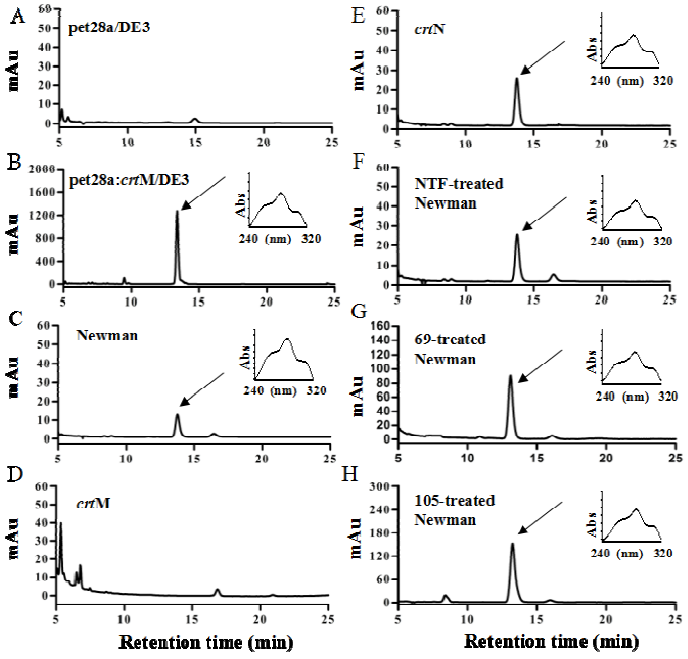

Figure 4. Effects of **69** and **105** on susceptibility to hydrogen peroxide killing. *S. aureus* Newman (A), USA400 MW2 (B), USA300 LAC (C), and Mu50 (D); *** $p <$ 0.001 via two-tailed t-test (n = three biological replicates, each with two technical replicates).

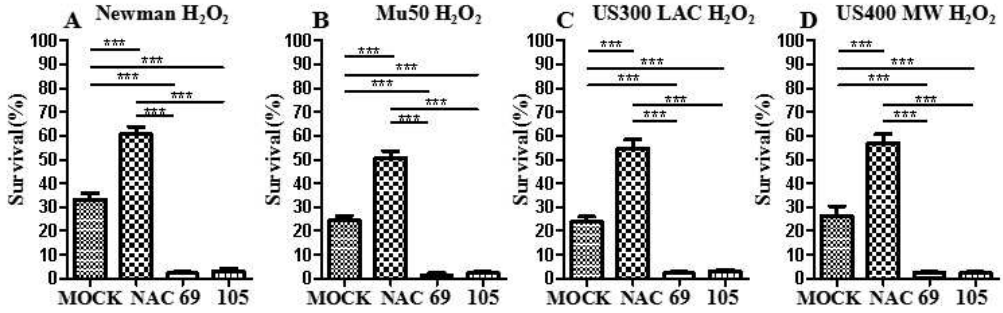

Figure 5. Effects of **69** and **105** on susceptibility to human whole blood killing. *S. aureus* Newman (A), USA400 MW2 (B), USA300 LAC (C), and Mu50 (D); *** p < 0.001 via two-tailed t-test (n = three biological replicates, each with two technical replicates).

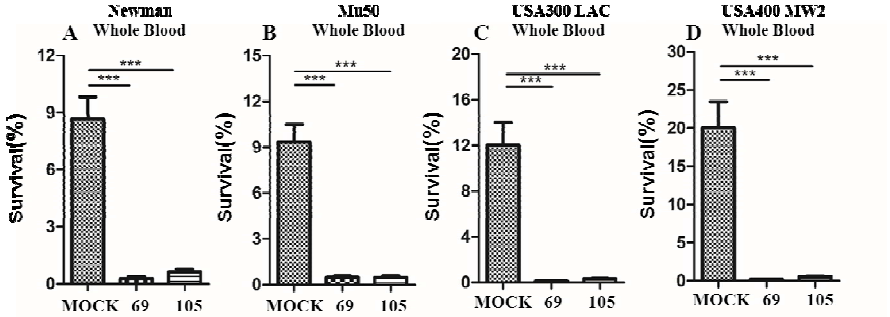

Figure 6. Effects of derivatives **69** (in blue) and **105** (in red) on *S. aureus* bacteria survival in the hearts (A) and livers (B) of mice (n=10 for each group) challenged with 2.3×10^7 CFU of Newman bacteria. **P** = pretreatment, drugs or compounds were intraperitoneally administered 24hours before infection, compared with the normal treatment (drugs or compounds were administered 6 hours after infection). Statistical significance was determined by the Mann-Whitney test (two-tailed): *** $p < 0.001$, n.s. indicates no significant difference. Each symbol represents the value for an individual mouse. Horizontal bars indicate the observation means, and dashed lines mark the limits of detection.

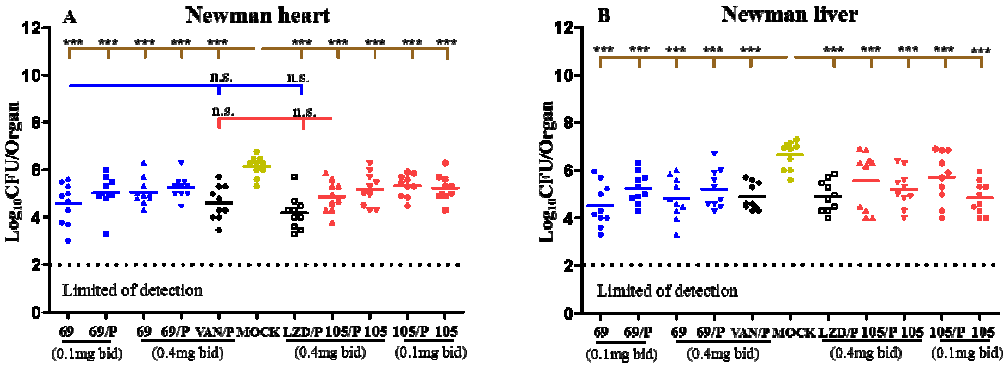

Figure 7. Effects of derivatives **69** (in blue) and **105** (in red) on *S. aureus* bacteria survival in the hearts (A) and livers (B) of mice (n=10 for each group) challenged with 1.1×10^9 CFU Mu50 bacteria. **P** = pretreatment, drugs or compounds were intraperitoneally administered 24 hours before infection, compared with the normal treatment (drugs or compounds were administered 6 hours after infection). Statistical significance was determined by the Mann-Whitney test (two-tailed): * $p < 0.05$, ** $p < 0.01$, *** $p < 0.001$, n.s. indicates no significant difference. Each symbol represents the value for an individual mouse. Horizontal bars indicate the observation means, and dashed lines mark the limits of detection.

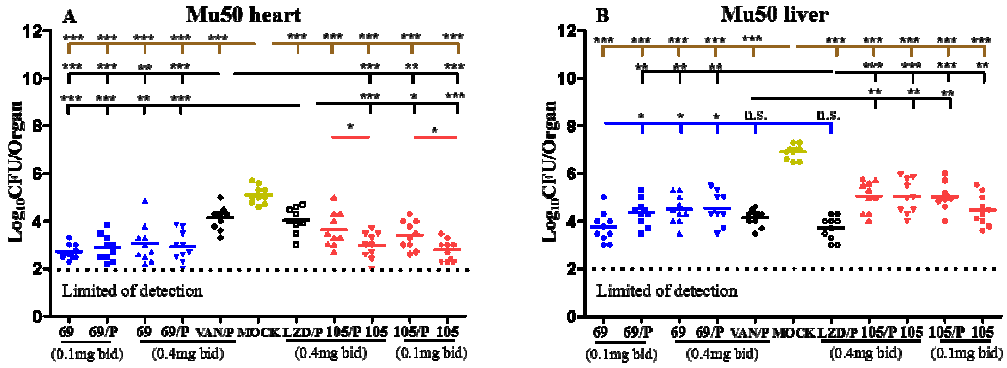

Figure 8. Effects of derivatives **69** (in blue) and **105** (in red) on *S. aureus* bacteria survival in the hearts (A) and livers (B) of mice (n=10 for each group) challenged with 1.9×10^8 CFU of NRS271 bacteria. **P** = pretreatment, drugs or compounds were intraperitoneally administered 24 hours before infection, compared with the normal treatment (drugs or compounds were administered 6 hours after infection). Statistical significance was determined by the Mann-Whitney test (two-tailed): ** $p < 0.01$, *** $p < 0.001$, n.s. indicates no significant difference. Each symbol represents the value for an individual mouse. Horizontal bars indicate the observation means, and dashed lines mark the limits of detection.

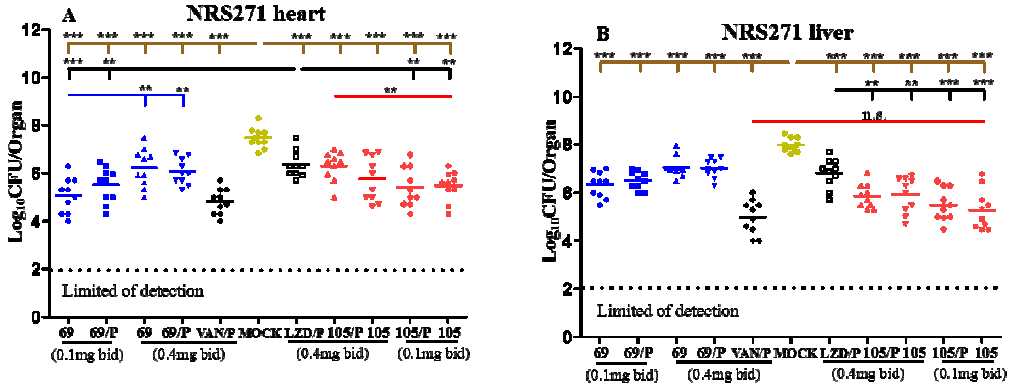

SCHEMES

Scheme 1. Syntheses of Derivatives **11-86**[a]

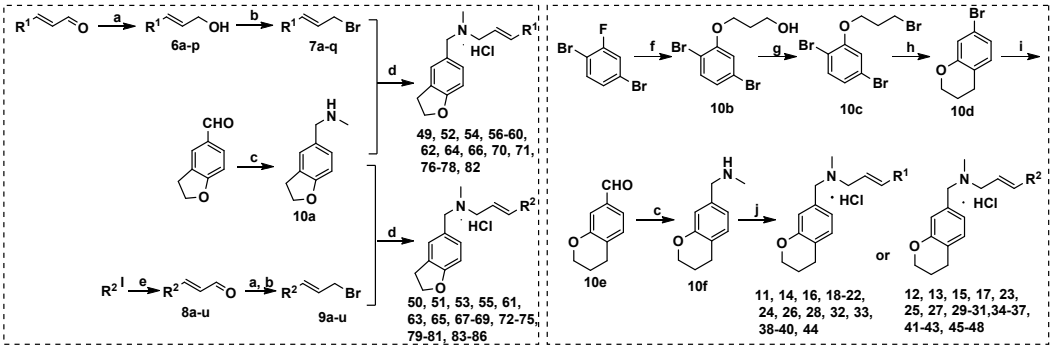

7q (allyl bromide), **11, 49** R^1 = H
6a, 7a, 14, 52 R^1 = furan-2-yl
6b, 7b, 16, 54 R^1 = 1-naphthyl
6c, 7c, 18, 56 R^1 = phenyl
6d, 7d, 19, 57 R^1 = 4-fluorophenyl
6e, 7e, 20, 58 R^1 = 4-chlorophenyl
6f, 7f, 21, 59 R^1=4-bromophenyl
6g, 7g, 22, 60 R^1=4-methylphenyl
6h, 7h, 24, 62 R^1=4-trifluoromethylphenyl
6i, 7i, 26, 64 R^1=4-methoxylphenyl
6j, 7j, 28, 66 R^1=4-nitrophenyl
6k, 7k, 32, 70 R^1=2-fluorophenyl
6l, 7l, 33, 71 R^1=2-chlorophenyl
6m, 7m, 38, 76 R^1=3-fluorophenyl
6n, 7n, 39, 77 R^1=3-chlorophenyl
6o, 7o, 40, 78 R^1=3-methylphenyl
6p, 7p, 44, 82 R^1=2,4-dichlorophenyl
8a, 9a, 12, 50 R^2=cyclopentyl
8b, 9b, 13, 51 R^2=cyclohexyl
8c, 9c, 15, 53 R^2=2-thienyl
8d, 9d, 17, 55 R^2=2-naphthyl
8e, 9e, 23, 61 R^2=4-difluoromethylphenyl
8f, 9f, 25, 63 R^2=4-*t*-butylphenyl
8g, 9g, 27, 65 R^2=4-ethoxylphenyl
8h, 9h,29, 67 R^2=4-cyanphenyl
8i, 9i, 30, 68 R^2=4-formate-(methyl)-phenyl
8j, 9j, 31, 69 R^2=4-biphenyl
8k, 9k, 34, 72 R^2=2-methylphenyl
8l, 9l, 35, 73 R^2=2-trifluoromethylphenyl
8m,9m, 36, 74 R^2=2-nitrophenyl
8n, 9n, 37, 75 R^2=2-methoxylphenyl
8o, 9o, 41, 79 R^2=3-trifluoromethylphenyl
8p, 9p, 42, 80 R^2=3-nitrophenyl
8q, 9q, 43, 81 R^2=3-methoxylphenyl
8r, 9r, 45, 83 R^2=2-fluoro-4-trifluoromethylphenyl
8s, 9s, 46, 84 R^2=3-fluoro-4-trifluoromethylphenyl
8t, 9t, 47, 85 R^2=2-fluoro-4-methoxylphenyl
8u, 9u, 48, 86 R^2=3-fluoro-4-methoxylphenyl

[a]Reagents and conditions: (a) $NaBH_4$, MeOH, 0 ºC, 1 h; (b) PBr_3, Et_2O, 0 ºC, 10 min; (c) (1) 30% methylamine in methanol, r.t., 2 h; (2) NaBH4, MeOH, 0 ºC, 1 h; (d) (1) K_2CO_3, DMF, r.t., 1 h; (2) HCl gas, Et_2O, r.t., 5 min. (e) (1) 3, 3-dimethoxy-1-propene, K_2CO_3, KCl, $Pd(OAc)_2$, PPh_3, THF, 60 ºC,4 h; (2) 5% hydrochloric acid, r.t., 2 h; (f) 1,3-propanediol, *tert*-BuOK, 1-methyl-2-pyrrolidinone, 100 ºC, overnight; (g) phosphorous tribromide, toluene, reflux, 4 h; (h) *n*-BuLi, THF / n-hexane(2:1), -70 ºC, 4 h; (i) n-BuLi, DMF, THF / n-hexane(2:1), -70 ºC, 2 h; (j) (1) **7a-q** or **9a-u**, K_2CO_3, DMF, r.t., 1 h; (2) HCl gas, Et_2O, r.t., 5 min.

Scheme 2. Syntheses of Derivatives **89-94**[a]

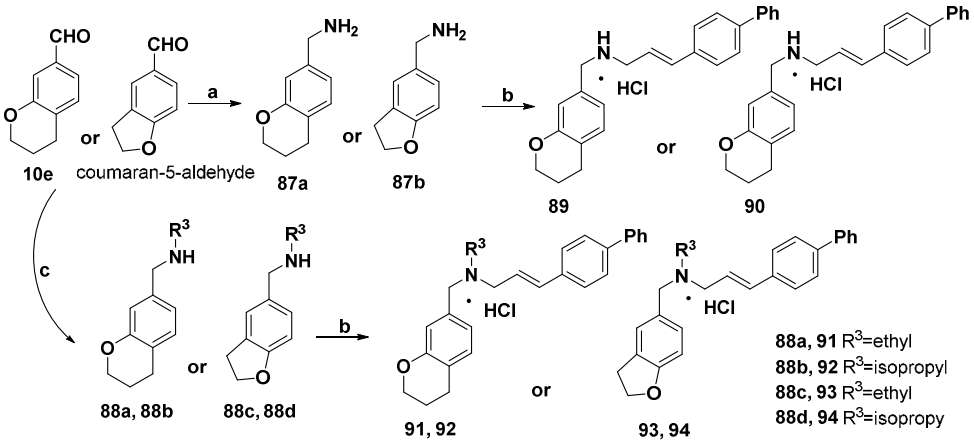

[a]Reagents and conditions: (a) (1) hydroxylammonium chloride, NaOH, water/enthol (1:3), 40 ºC, 3 h; (2) $Pd(OH)_2$, H_2, MeOH, r.t., overnight; (b) (1) **9j**, K_2CO_3, DMF, r.t., 1 h; (2) HCl gas, Et_2O, 5 min; (c) (1) ethylamine or isopropylamine, r.t., 2 h; (2) $NaBH_4$, MeOH, 0 ºC, 1 h.

Scheme 3. Syntheses of Derivatives **100-109**[a]

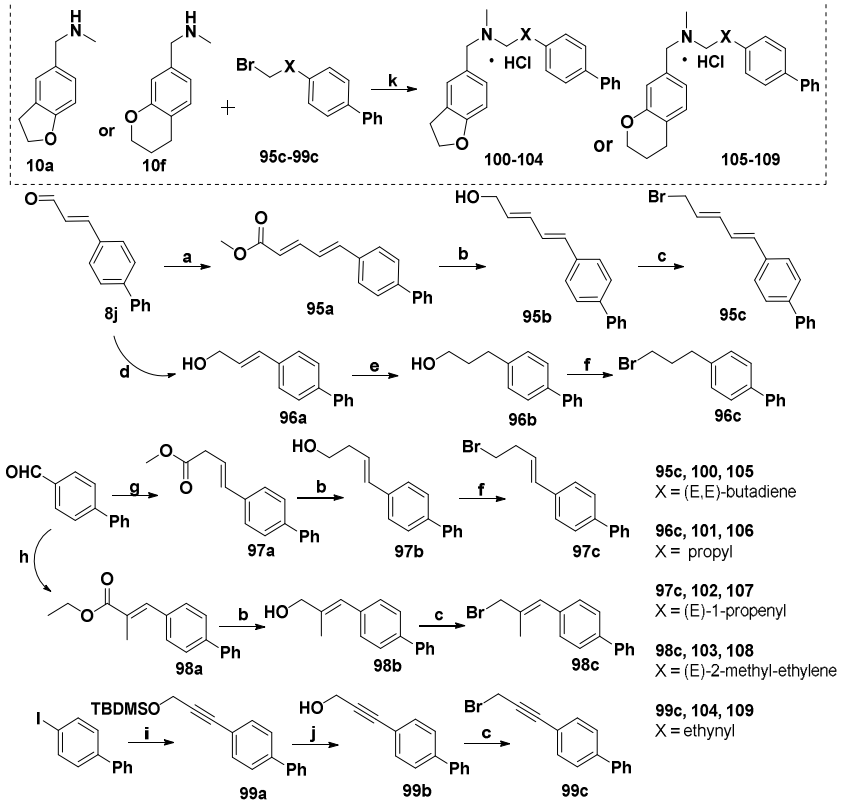

[a]Reagents and conditions: (a) methyl (triphenylphosphoranylidene) acetate, toluene, 100 ºC, 1 h; (b) DIBAL-H, THF, 0 ºC, 6 h; (c) PBr_3, Et_2O, 0 ºC, 5 min; (d) $NaBH_4$, MeOH, rt, 1h; (e) Pd / C, H_2, MeOH, overnight; (f) CBr_4, PPh_3, CH_2Cl_2, r.t., 1 h; (g) (1) (2-carboxyethyl)triphenylphosphonium bromide, NaH, toluene, 100 ºC, 1 h; (2) $SOCl_2$, MeOH, reflux, 3 h; (h) ethyl(1-methyl-triphenylphosphoranylidene)acetate, toluene, 100 ºC, 1 h; (i) O-TBDMS-2-propyny-1-ol, CuI, $Pd(PPh_3)_4$, Et_3N, DMF, 80 ºC, 6 h; (j) tetrabutylammonium fluoride, THF, 0 ºC, 1 h; (k) (1) K_2CO_3, DMF, r.t., 1 h; (2) HCl gas, Et_2O, rt, 5 min.

TABLES

Table 1. Chemical Structures of Derivatives **11-86** and Their Pigment Inhibitory Activities against *S. aureus* Newman

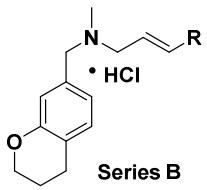

Series B

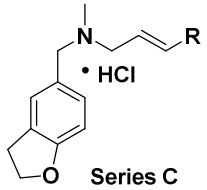

Series C

Compd. (B / C)	R	IC_{50} (nM)[a] (Series B)	IC_{50} (nM)[a] (Series C)	Compd. (B / C)	R	IC_{50} (nM)[a] (Series B)	IC_{50} (nM)[a] (Series C)
11/49		>1000	>1000	**30/68**	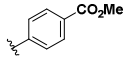	5.9±1.6	20.4±2.9
12/50		>1000	>1000	**31/69**	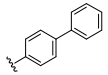	3.8±0.1	2.2±0.5
13/51		>1000	253.6±1.4	**32/70**		>1000	564.6±76.9
14/52		>1000	>1000	**33/71**		>1000	>1000
15/53		>1000	>1000	**34/72**		>1000	>1000
16/54		>1000	>1000	**35/73**		463.6±90.5	>1000
17/55	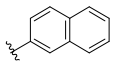	5.2±0.4	5.2±1.4	**36/74**		>1000	>1000

18/56		>1000	>1000	**37/75**		>1000	>1000
19/57	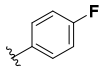	>1000	43.4±3.5	**38/76**	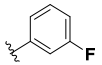	141.6±0.6	>1000
20/58	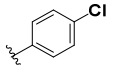	9.0±1.3	>1000	**39/77**	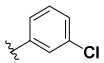	654.4±20.4	>1000
21/59	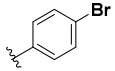	4.8±0.5	12.4±6.8	**40/78**		400.4±17.1	>1000
22/60	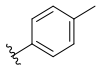	6.5±0.0	29.0±10.9	**41/79**	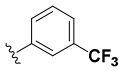	642.4±229.6	238.6±32.8
23/61	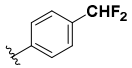	4.5±0.1	5.2±1.8	**42/80**	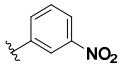	>1000	>1000
24/62	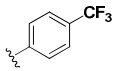	4.6±0.1	2.1±0.2	**43/81**	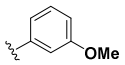	>1000	>1000
25/63	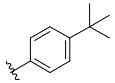	>1000	17.8±0.1	**44/82**	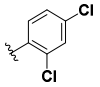	>1000	>1000
26/64	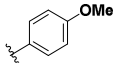	16.0±0.8	33.5±4.9	**45/83**	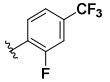	4.7±0.4	5.8±0.1
27/65		9.9±0.4	6.9±0.5	**46/84**		8.7±0.4	49.0±2.5
28/66		>1000	>1000	**47/85**	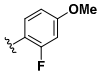	5.9±0.4	24.5±1.0

29/67		12.3±1.1	27.3±3.0	**48/86**	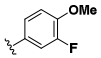	54.4±3.6	>1000

[a]The values given are the IC_{50} values for pigment inhibition in *S. aureus* Newman. The values are reported as the average ± S.D.

Table 2. Chemical Structures of Derivatives **89-94** and Their Pigment Inhibitory Activities against *S. aureus* Newman

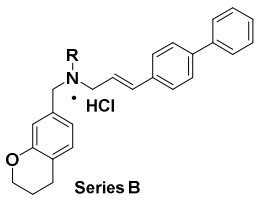

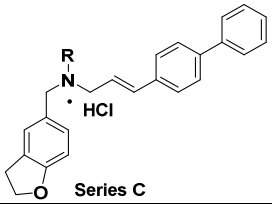

compd (B / C)	R	IC_{50} (nM)[a] (Series B)	IC_{50} (nM)[a] (Series C)
89/90	**H**	>1000	>1000
91/93		>1000	256.5±11.5
92/94		>1000	>1000

[a]The values given are the IC_{50} values for pigment inhibition in *S. aureus* Newman. The values are reported as the average ± S.D.

Table 3. Chemical Structures of Derivatives **100-109** and Their Pigment Inhibitory Activities against *S. aureus* Newman

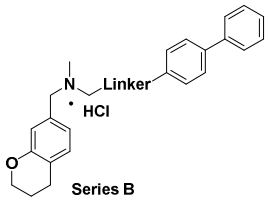

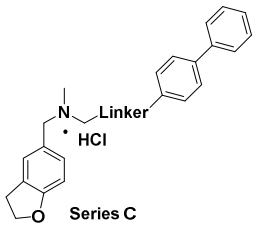

Linker	Compd. (B / C)	IC_{50} (nM)[a] (Series B)	IC_{50} (nM)[a] (Series C)
105/100	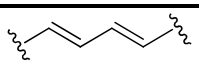	3.0±0.4	7.7±0.3
106/101	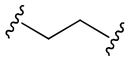	>1000	>1000
107/102	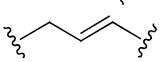	>1000	>1000
108/103	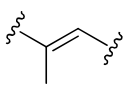	17.3±0.2	23.5±0.8
109/104	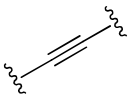	>1000	>1000

[a]The values given are the IC_{50} values for pigment inhibition in *S. aureus* Newman. The values are reported as the average ± S.D.

Table 4 Chemical Structures of Derivatives Selected and Their Water Solubility and hERG Inhibitory Activities

compd	Water Solubility (mg/mL)[a]	hERG IC_{50}(μM)[b]	compd	Water Solubility (mg/mL)[a]	hERG IC_{50}(μM)[b]
17	2.2	16.2	**55**	2.6	6.7
23	16.3	1.9	**61**	18.5	1.3
24	13.2	2.9	**62**	14.6	2.2
27	10.2	-	**65**	11.6	-
31	3.7	32.1	**69**	4.4	11.3
45	15.2	3.2	**83**	16.3	2.9
20	11.5	-	**30**	5.6	6.5
21	16.4	1.9	**46**	16.8	0.2
22	6.3	3.8	**47**	13.1	3.1
4	4.1	1.4	**5**	0.7	3.2
4a[c]	0.6	-	**5a**[c]	2.0	-
4b[c]	1.2	-	**5b**[c]	1.9	-
4c[c]	1.4	-	**5c**[c]	0.9	-
4d[c]	2.6	-	**105**	3.8	>40

[a]The values given are the solubility in water, in mg/mL. [b]The values given are the IC_{50} values for hERG inhibition, in μM. [c]The structure of compounds had been reported in ref. 31, and were shown again in Figure S5 in *Supporting Information*.

Table 5. Enzyme (CrtN IC_{50}), Pigment (*S.aureus* Newman, Mu50, NRS271, USA400 MW2, USA300LAC, NF65Y, LRSA56 IC_{50}) Results of Four Representative Derivatives.

compd	CrtN IC_{50} (nM)[a]	*S.aureus* Newman IC_{50}(nM)[b]	Mu50 IC_{50} (nM)[b]	NRS271 IC_{50}(nM)[b]	USA400 MW2 IC_{50}(nM)[b]	USA300 LAC IC_{50}(nM)[b]	NF65Y IC_{50}(nM)[b]	LRSA56 IC_{50}(nM)[b]
31	213.2±37.8	3.8±0.1	1.3±0.2	2.0±0.3	9.2±0.5	9.5±0.5	-	-
62	230.6±25.6	2.1±0.2	2.2±0.2	2.2±0.2	9.0±0.4	8.1±1.0	-	-
69	181.3±34.3	2.2±0.5	0.33±0.3	0.4±0.1	6.3±0.5	8.8±0.5	1.2±0.1	2.2±0.3
105	179.6±29.5	3.0±0.4	0.36±0.1	1.3±0.2	7.4±0.3	13.1±1.2	1.0±0.1	1.7±0.1
4	320	4.07	0.49	-	7.08	7.65	-	-

[a]The values given are the IC_{50} values against CrtN, in nM. [b]The values given are the IC_{50} values for pigment inhibition in *S. aureus* Newman, NRS271, USA400 MW2 and USA300 LAC, in nM. The values are reported as the average ± S.D.

Table 6. Pharmacokinetic Characterization of **69** with Either IV or PO Injection in Intact Rats

69	$T_{1/2}$ (h)	T_{max} (h)	C_{max} (ng/mL)	$AUC_{(0-t)}$ (h*ng/mL)	$AUC_{(0-\infty)}$ (h*ng/mL)	$MRT_{(0-t)}$ (h)	$MRT_{(0-\infty)}$ (h)	F (%)
IV (5 mg/kg)	2.27	0.083	2044.71	1331.84	1362.33	0.90	1.13	-
SD (*n* = 3)	0.30	0.000	123.69	48.30	54.14	0.06	0.10	-
PO (10 mg/kg)	1.70	2.00	41.78	156.46	177.02	2.61	3.28	6.50
SD (n = 3)	0.19	0.00	10.16	41.47	49.56	0.02	0.19	1.82

Table 7. Antifungal Activity of Derivatives **69 and 105**

compd	antifungal activity MIC (μg/mL)		
	Trichophyton rubrum	*Microsporum gypseum*	*Tinea barbae*
69	16	16	16
105	> 64	> 64	> 64
ketoconazole	0.25	0.25	16
voriconazole	0.03	0.25	0.125
fluconazole	0.5	8	2

Table 8. The Solubilities of Salt **69a-j** and **105a-j**

Compd.	Salt type	Water Solubility (mg/mL)[c]		Compd.	Salt type	Water Solubility (mg/mL)[c]	
69a/105a	sulfate[a]	1.8	1.1	**69f/105f**	lactate[b]	6.2	6.5
69b/105b	phosphate[a]	16.2	12.9	**69g/105g**	succinate[b]	3.3	2.3
69c/105c	hydrobromate[a]	2.2	2.8	**69h/105h**	tartrate[b]	5.7	4.6
69d/105d	acetate[b]	4.7	4.1	**69i/105i**	maleate[b]	1.2	1.3
69e/105e	trifluoroacetate[a]	1.5	1.7	**69j/105j**	citrate[b]	2.3	1.6

[a]The condition of salt formation according to General Procedure A for preparation of salts. [b]The condition of salt formation according to General Procedure B for preparation of salts. [c]The values given are the solubility in water, in mg/mL.

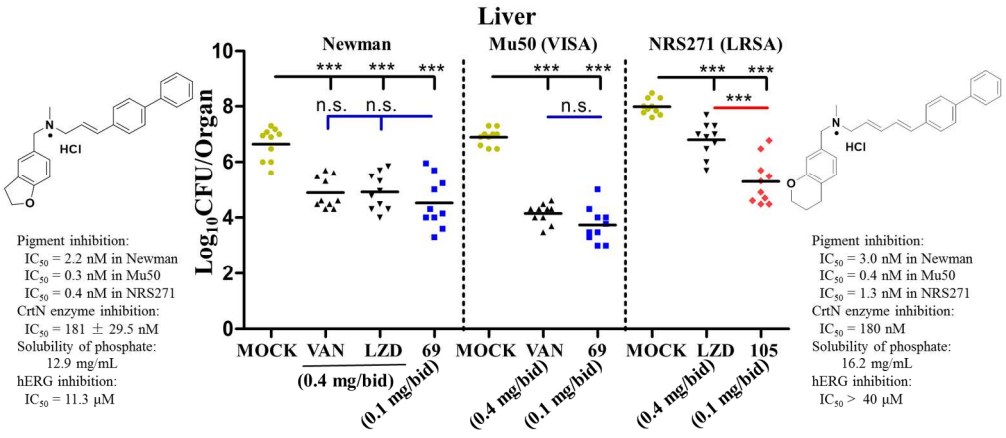

Table of Contents graphic

387x176mm (130 x 130 DPI)